Journal of ELECTRONIC MATERIALS, Vol. 45, No. 8, 2016
DOI: 10.1007/s11664-016-4623-1

$(Ba_{0.85}Ca_{0.15})(Zr_{0.1}Ti_{0.9})O_3$ Ceramics Synthesized by a Gel-Casting Method

WEI XIONG[1,2]

1.—Department of Materials, Imperial College London, London SW7 2AZ, UK. 2.—e-mail: wx1315@ic.ac.uk

$(Ba_{0.85}Ca_{0.15})(Zr_{0.1}Ti_{0.9})O_3$ (BCZT) powder was synthesized by a solid-state reaction method, then the ceramics were fabricated by gel-casting and die-pressing routes, respectively. Piezoelectric coefficient (d_{33}) was measured by the $d_{33\ m}$; Planar mode electromechanical coupling coefficient (k_p), dielectric loss ($tan\delta$) and relative permittivity (ε_r) were measured by the impedance analyzer. Results of measurements showed that in the range of tested sintering temperature (1300–1500°C), gel-casting samples showed better piezoelectric and electromechanical coupling coefficients (d_{33} = 395 pC/N, k_p = 0.44) compared with die-pressing samples, and comparable dielectric properties were also observed. ($tan\delta$ = 0.037, ε_r = 3267).

Key words: BCZT, gel-casting, piezoelectric properties, dielectric properties

INTRODUCTION

Lead zirconate titanate (PZT) has been the most successful piezoelectric ceramic for decades. It is used in various actuators and transducers,[1–3] and it has excellent piezoelectric properties compared with other piezoelectric ceramics. However, a concern over PZT's environmental impact has emerged in recent years due to the high toxicity of its lead content. Therefore, a continual search for a more environmentally friendly piezoelectric materials is carried out around the world, particularly as the European Union issued a directive that limits the potential use of PZT in applications.[4] $(Ba_{0.85}Ca_{0.15})(Zr_{0.1}Ti_{0.9})O_3$ (BCZT) is a type of lead-free material with a perovskite structure. Compared with many other lead-free candidates which possess a low piezoelectric coefficient (d_{33}), such as bismuth sodium titanate (BNT; d_{33} = 64 pC/N)[5] and CuO-added $KNbO_3$ (xCKN; d_{33} = 65–110 pC/N).[6] BCZT was reported in many papers to have excellent piezoelectric properties (d_{33} = 560–620 pC/N)[7] that are even comparable to some high-end PZT compounds.[8]

The effects of doping, synthesis methods and sintering temperature have been extensively studied worldwide to develop the high performances in BCZT systems, yet little has been done to investigate the gel-casting method, which is considered as a new technique of fabricating the fine-scale piezoelectric ceramic structures. This technique is required for the 1-3 piezocomposite fabrication, which is the preferred active material in the high-frequency transducers that exhibit excellent performances.[9] It is characterized by casting the slurry into moulds with desired shapes followed by the polymerization reactions that form a rigid gel, and this slurry is a mixture of ceramic powders, distilled water, dispersant and organic monomers. Gel-casting has been widely accepted by the industries when fabricating ceramics with complex shapes. It addresses the issue of density difference and requires inexpensive resources compared with other conventional methods like injection moulding. Favorable mechanical properties, complex shape production and versatility for both metal and ceramic powders can also be achieved by using the gel-casting method.[10] Despite these advantages, previous researches seldom focus on the effects of gel-casting on the piezoelectric and dielectric properties of BCZT systems, but more on PZT systems.[11] In this paper, the enhanced piezoelectric properties and comparable dielectric properties of BCZT ceramics produced by a gel-casting technique are achieved in a range of sintering temperatures.

(Received January 24, 2016; accepted May 3, 2016; published online May 13, 2016)

EXPERIMENTAL

Solid-State Reaction and Die-Pressing

The raw materials used were $BaCO_3$ (99.98%, Dakram Materials Ltd, UK), $CaCO_3$ (99.4%, Lach-Ner, Ltd., Czech Republic), ZrO_2 (99.82%) and TiO_2 (99.9%, PI-KEM Ltd, UK). Two batches of mixed powders (labeled as batch A and batch B) were prepared with 100.0817 g per batch (62.8467 g $BaCO_3$, 5.6578 g $CaCO_3$, 4.6243 g ZrO_2 and 26.9529 g TiO_2). This was determined by calculating the needed amount to achieve stoichiometry of $(Ba_{0.85}Ca_{0.15})(Zr_{0.1}Ti_{0.9})O_3$. The powders were then wet-milled with 200 g of zirconia balls using the ball-milling machine for 12 h. After being dried in an oven at 80°C for 24 h, the two batches of powders were calcined at 1250°C for 2 h. A small amount of the powders were taken for x-ray diffraction (XRD) characterization. And then the rest of them were ball-milled again with distilled water and zirconia balls for 24 h. DURAMAX B-1000 and B-1007 (Dow Chemical, UK) were added into batch A after milling as binders and the mixture was further milled for 20 min, and the milled powders of batch A (with binders) and B (without binders) were dried in an oven at 90°C for 24 h as raw materials for the die-pressing and gel-casting routes, respectively. Powder of batch A was pressed into pellets with a diameter of 13 mm using an Instron 5507 mechanical testing machine (Instron, UK). A uniaxial pressing load of 12.5kN was applied for 1 min. Then, these pressed pellets were divided into 3 groups (5 samples each) that were sintered separately at 3 different temperatures: 1300°C, 1400°C and 1500°C. The sintering of the die-pressing samples started from 40°C and the temperature was firstly increased to 325°C and then 500°C and held for 1 h, respectively; this is to burn out the binders added before. The samples were then sintered at the corresponding sintering temperatures for 4 h.

Gel-Casting

Calcined powder of batch B (without DURAMAX binders) was used. 1 g of hydantoin epoxy resin (Hubei Xital Chemical Co., Ltd, China) was mixed with 4 g of distilled water to make a premix solution, and then it was mixed with zirconia balls and 0.5907 g of a dispersant agent (Dispex AA4040, BASF, UK). 24.6119 g of powder was then added to make a slurry, which was done in three divided times (12 g, 6 g, 6.6119 g each time), and then the powder was wet-milled in the ball-milling machine for 20 min each time the powder was added. After milling, the slurry was mixed with Bis(3-aminopropyl)amine (Sigma-Aldrich, Germany) as a hardener. Evacuation of the slurry was carried out before and after adding a hardener by using a vacuum desiccator for around 2 min in order to eliminate bubbles inside the slurry, and then the slurry was cast in the polydimethylsiloxane (PDMS) moulds, which have a diameter of around 13 mm and thickness of 4–5 mm. The moulds containing the cast samples were dried at room temperature for 24 h and then dried in an oven at 40°C for 24 h to achieve BCZT green bodies. Finally, they were put in a furnace to go through the same sintering profile as die-pressing samples.

Characterization

The density (ρ) of the sintered samples was measured by the Archimedes method using distilled water. The sintered samples of both fabrication routes were coated with gold as electrodes on their plain surfaces and then poled in a silicon oil bath with an applied electric field of 3kv/mm at room temperature for 10 min, and their piezoelectric and dielectric properties were measured 24 h after poling. XRD characterization (Cu-$K_{\alpha 1}$ radiation, λ = 1.5406Å) of the calcined powder and sintered samples at three different temperatures were carried out using the XER diffractometer (Philips X'pert). Scanning electron microscopy images (SEM JSM 6060) were taken on the plain surface of the green bodies and sintered samples in both fabrication routes after cleaning the surfaces. d_{33} was measured using a $d_{33\ m}$ (SINOCERA, Shanghai, China). A resonance–antiresonance method was applied to measure planar mode electromechanical coupling coefficients (k_p). Capacitance, relative permittivity (ε_r) and dielectric loss ($tan\delta$) values were measured by using the Agilent 4294A impedance analyzer (Agilent Ltd, UK).

RESULTS AND DISCUSSION

XRD Pattern

The XRD patterns of 1250°C-calcined powder as well as 1300°C-, 1400°C- and 1500°C-sintered ceramics of the die-pressing fabrication route are shown in Fig. 1.

Featured peaks of BCZT are labeled with the Miller index, and impurity peaks that are identified in the XRD pattern of the 1250°C-calcined powder were marked with black lines. These impurities could be un-calcined raw ceramic powders like $CaCO_3$ and ZrO_2; or could be the by-products after calcination such as $CaTiO_3$. It is notable that there are no impurity peaks identified in the XRD patterns of any sintered ceramics, implying that the impurity phases were eliminated during sintering and a pure perovskite structure was formed. However, it can be seen that the increased sintering temperature have no apparent influence on the position of the relative intensities of the XRD patterns of the corresponding samples, which indicates that different sintering temperatures do not change the phase structure of BCZT significantly.

Density

The density (g/cm^3) of the sintered ceramics is listed in Table I. Each datum is recorded by calculating the average value of samples sintered at the same temperature and fabrication route, together with the standard deviation values.

The density of sintered ceramics almost remains constant when the temperature goes up and no extant change is identified comparing the two fabrication methods. Gel-casting samples show the same change as observed in the literature[8] (decreasing then increasing slightly). But overall, the tested sintering temperature does not affect density of the BCZT sample greatly, and this may be because in the BCZT system, densification is already completed before reaching 1300°C.

Piezoelectric and Dielectric Properties

Piezoelectric properties, including d_{33} (pC/N) and k_p, together with dielectric properties, including $tan\delta$ and ε_r, of the sintered BCZT samples are presented in Table I.

From Table I, some results can be identified. Firstly, d_{33} increased in both die-pressing and gel-casting samples when the sintering temperature was raised from 1300°C to 1400°C, and kept increasing but with a slower rate in gel-casting samples when temperature went up from 1400°C to 1500°C. Although this value of the 1500°C-sintered die-pressing sample was reduced a little, it was still very close to that of the 1400°C sample. It is clear that gel-casting samples overall had higher d_{33} values than die-pressing samples at the same temperature. It is also notable that the deviations of gel-casting samples were relatively higher, which is possibly because of the inhomogeneous compositions in each sample caused by the highly viscous slurry during the process of preparing and casting. But, the general d_{33} values of gel-casting samples were still better even considering the deviation. Comparing with the literature[8] with the same BCZT composition (d_{33} = 650 pC/N at 1540°C sintering temperature), much lower value (d_{33} = 396 pC/N for the gel-casting sample at 1500°C) was obtained in this work. The sintering temperature here was generally lower than that in the literature (1520–1540°C).

Secondly, the k_p value increased when elevating temperature from 1300°C to 1400°C, and then

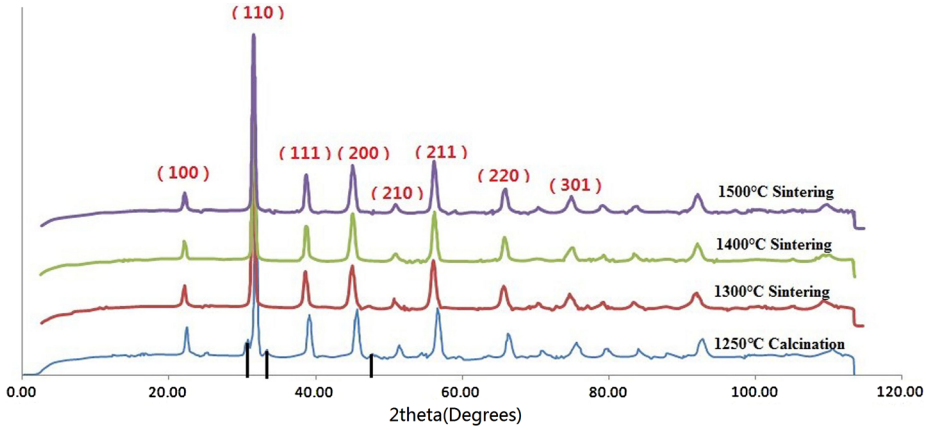

Fig. 1. XRD pattern of calcined powder at 1250°C and subsequent sintered ceramics at 1300°C, 1400°C and 1500°C.

Table I. Properties of die-pressing and gel-casting samples

Temperature (°C)	1300	1400	1500
Die-pressing			
ρ (g/cm^3)	5.47 ± 0.05	5.63 ± 0.17	5.54 ± 0.06
d_{33} (pC/N)	76 ± 9.35	352 ± 19.52	344 ± 26.48
k_p	0.17 ± 0.03	0.41 ± 0.02	0.38 ± 0.05
$tan\delta$	0.044 ± 0.002	0.039 ± 0.004	0.035 ± 0.009
ε_r	2980.23 ± 142.34	3394.16 ± 293.76	3116.17 ± 207.18
Gel-casting			
ρ (g/cm^3)	5.60 ± 0.11	5.48 ± 0.15	5.58 ± 0.12
d_{33} (pC/N)	138 ± 25.32	370 ± 64.63	396 ± 46.24
k_p	0.23 ± 0.04	0.44 ± 0.05	0.44 ± 0.04
$tan\delta$	0.046 ± 0.008	0.049 ± 0.010	0.037 ± 0.005
ε_r	3010.51 ± 216.03	3151.70 ± 133.95	3267.88 ± 272.52

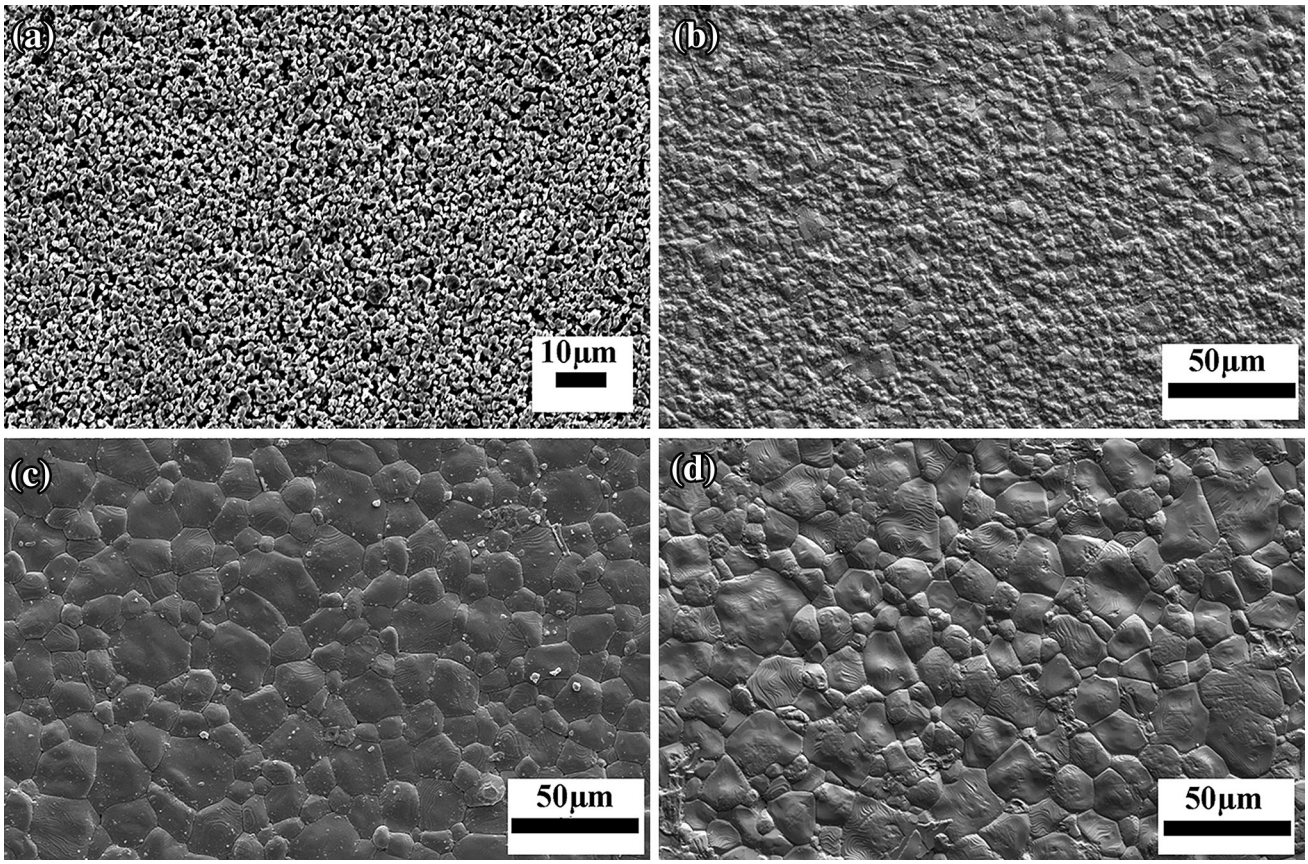

Fig. 2. Plain surface SEM image of (a) gel-casting green body (b) 1300°C-sintered gel-casting (c) 1400°C-sintered gel-casting (d) 1500°C-sintered gel-casting.

decreased to a small extent after 1400°C. Gel-casting samples generally showed higher k_p values compared with die-pressing ones.

Thirdly, the overall trend of $tan\delta$ values of the samples decreased when the sintering temperature was increased from 1300°C to 1500°C. Comparing the gel-casting and die-pressing samples, lower $tan\delta$ values were observed in die-pressing samples, but the difference was small, especially at 1300°C and 1500°C.

As for relative permittivity, as shown in Table I, the ε_r value of sintered gel-casting samples increased steadily when sintering temperature was changed from 1300°C to 1500°C, whereas that of die-pressing ones dropped above 1400°C. However, the values were also quite similar for both fabrication routes (ε_r = 3100–3200 at 1500°C).

It is notable that the superior piezoelectric properties of gel-casting samples was also observed in the PZT system by carefully choosing the dispersant content, although the advantage was relatively small.[12,13]

Microstructure

The SEM images of the plain surface of the BCZT green bodies and sintered samples are presented in Fig. 2. The sample surface was grounded roughly to clean most dust and impurities before doing SEM.

It can be seen from Fig. 2b–d that the low sintering temperature of 1300°C resulted in smaller grain size, and the grain boundaries became unclear and hard to differentiate. The grain size increased with elevated sintering temperature, which coincides with previous literature.[14] Roughly estimated, the grain size was much larger than 10 μm at high temperatures, whereas in other systems, like KNN, it was only 3 μm.[15] This is possibly because this temperature satisfies the need of grain growth in the BCZT system but is not adequate for that of a KNN system due to the volatilization of K_2O at such temperature.[8] This large-grain microstructure at high temperature and the positive correlation between sintering temperature and grain size in BCZT system coincides with the literature, and the controlling effect of sintering temperature on grain size was observed. Another notable thing is that relating the grain size with previous d_{33} property, the d_{33} values were very low at low sintering temperatures, where there were no large grains. This characteristic fits what was found in the literature,[8,16] that d_{33} was markedly influenced by grain sizes.

CONCLUSION

Lead-free piezoelectric ceramic BCZT was synthesized by both conventional die-pressing and advanced gel-casting samples. Different sintering temperatures did not change the phase structure of BCZT and similar densities were shown. However, they greatly influenced the grain size, piezoelectric coefficient d_{33} and planar mode electromechanical coupling coefficient k_p.

Both d_{33} and k_p were improved by using the gel-casting method, which is also observed in previous reports of PZT systems. But the dielectric losses of die-pressing samples were lower. Gel-casting and die-pressing samples demonstrated similar relative permittivity, and the densities of gel-casting samples were also quite close to die-pressing ones, which could be due to the fact that the BCZT system requires less temperature to achieve densification.

In summary, compared with the die-pressing method, the gel-casting method not only has the advantage of being binder-free, but also showed better piezoelectric and electromechanical coupling coefficients in the BCZT system. These advantages make gel-casting a promising way of fabricating BCZT ceramics.

OPEN ACCESS

REFERENCES

1. D.-J. Shin, S.-J. Jeong, C.-E. Seo, K.-H. Cho, and J.-H. Koh, *Ceram. Int.* 41, 686 (2015).
2. C. Fei, Z. Chen, W.M. Fong, B. Zhu, L. Wang, W. Ren, Y. Li, J. Shi, K.K. Shung, and Q. Zhou, *Ceram. Int.* 41, 650 (2015).
3. Y. Yu, J. Wu, T. Zhao, S. Dong, H. Gu, and Y. Hu, *J. Alloys Compd.* 615, 676 (2014).
4. J. Rödel, W. Jo, K.T.P. Seifert, E.-M. Anton, and T. Granzow, *J. Am. Ceram. Soc.* 92, 1153 (2009).
5. P.K. Panda, *J. Mater. Sci.* 44, 5049 (2009).
6. J.-H. Kim, D.-H. Kim, I.-T. Seo, J. Hur, J.-H. Lee, B.-Y. Kim, and S. Nahm, *Sens. Actuators A* 234, 9 (2015).
7. W. Liu and X. Ren, *Phys. Rev. Lett.* 103, 257602 (2009).
8. P. Wang, Y. Li, and Y. Lu, *J. Eur. Ceram. Soc.* 31, 2005 (2011).
9. L. García-gancedo, S.M. Olhero, F.J. Alves, J.M.F. Ferreira, C.E.M. Demoré, S. Cochran, and T.W. Button, *J. Micromech. Microeng.* 22, 125001 (2012).
10. R. Gilissen, J.P. Erauw, A. Smolders, E. Vanswijgenhoven, and J. Luyten, *Mater. Des.* 21, 251 (2000).
11. D. Xu, X. Cheng, and H. Geng, *Ceram. Int.* 41, 9433 (2015).
12. D. Guo, K. Cai, L. Li, C. Nan, and Z. Gui, *Ceram. Int.* 29, 403 (2003).
13. D. Guo, K. Cai, L. Li, and Z. Gui, *J. Eur. Ceram. Soc.* 23, 1131 (2003).
14. S. Hunpratub, S. Maensiri, and P. Chindaprasirt, *Ceram. Int.* 40, 13025 (2014).
15. F. Rubio-Marcos, P. Marchet, T. Merle-Méjean, and J.F. Fernandez, *Mater. Chem. Phys.* 123, 91 (2010).
16. A. Yang, C.-A. Wang, R. Guo, Y. Huang, and C.-W. Nan, *Ceram. Int.* 36, 549 (2010).